

Graph Neural Networks with Haar Transform-Based Convolution and Pooling: A Complete Guide

Xuebin Zheng, Bingxin Zhou, *Student Member, IEEE*, Ming Li, *Member, IEEE*,
Yu Guang Wang, *Member, IEEE*, and Junbin Gao

Abstract—Graph Neural Networks (GNNs) have recently caught great attention and achieved significant progress in graph-level applications. In order to handle graphs with different features and sizes, we propose a novel graph neural network, which we call HAARNET, to predict graph labels with interrelated convolution and pooling strategies. Similar to some existing routines, the model assembles unified graph-level representations from samples by first adopting graph convolutional layers to extract mutual information followed by graph pooling layers to downsample graph resolution. By a sequence of clusterings, we embed the intrinsic topological information of each graph into the GNN. Through the fast Haar transformation, we made our contribution to forming a smooth workflow that learns multi-scale graph representation with redundancy removed. As a result, our proposed framework obtains notable accuracy gains without sacrificing performance stability. Extensive experiments validate the superiority on graph classification and regression tasks, where our proposed HAARNET outperforms various existing GNN models, especially on big data sets.

Index Terms—Graph Neural Network, Graph Pooling, Spectral Graph Convolution, Haar Wavelets, Coarse-grained Chain, Graph Classification, Graph Regression, Fast Haar Transforms.

I. INTRODUCTION

Graph representation learning has broad applications in network science, biology, physics, chemistry, medicine, robotics, computer vision, computer graphics and e-commerce [1]–[10]. Recently, graph neural networks (GNNs) have proved handy machinery for structured data representation and learning. They have become a topic of intense research due to their remarkable ability on graph data modelling tasks, including node classification, graph classification and regression, and link prediction [11]–[17]. In a GNN model, appropriate design of graph convolutional layers and pooling layers is crucial to the model to achieve excellent performance. In this paper, we develop graph convolution and pooling operations based on Haar wavelets on graphs, which can achieve a state of the art performance on graph classification and regression tasks.

Node classification and graph classification/regression are typical tasks on graph-structured data. The node classification

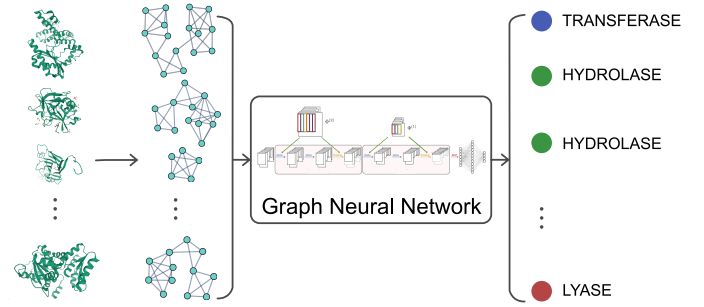


Fig. 1: An example of applying GNNs for labeling enzymes. A set of graphs is extracted as the input data set, where each graph represents a specific protein tertiary structure. The task is to assign each enzyme instance to one of the given EC top-level classes correctly. The GNN's role is to find universally applicable rules to label the graphs by learning the topological and feature information of the input. HAARNET provides a candidate GNN model with great potential. The structure of enzymes is retrieved from the Protein Data Bank [18].

works on a single input graph which is to predict unseen labels on nodes from labelled nodes. Its applications include relation inference, rating and recommendation of users for products, drug repurposing and so on [19]–[23]. The graph classification or regression is a task of predicting the unknown labels of individual input graphs from multiple labelled graphs. The size and structure of input graphs are possibly distinct from one to another. The applications of graph classification/regression include protein (i.e. enzyme) structure classification, point distribution pattern recognition in statistical physics, and atomization energy prediction in quantum chemistry [24]–[29].

Graph neural networks are useful for solving these problems. GNNs are deep neural networks with general architecture analogous to traditional CNNs except the input is graph-structured data. This difference, however, has a big impact on the construction of the network and its components, such as the counterparts of traditional convolution and pooling. In a GNN, graph convolution is an operation that can distil a geometric feature of the structured data which applies to both node-level and graph-level tasks. We develop a graph version of Fourier convolution using Haar wavelets for GNNs. The Haar-based convolution carries computations in Haar wavelet domain: the input feature on the graph and network filter are projected into the frequency domain by the forward Haar transform, and the convolution is then the adjoint Haar transform of the

X. Zheng, B. Zhou and J. Gao are with the Discipline of Business Analytics, The University of Sydney Business School, The University of Sydney, NSW, 2006 Australia (e-mail: {xuebin.zheng, junbin.gao}@sydney.edu.au, bzho3923@uni.sydney.edu.au). M. Li is with the Department of Educational Technology, Zhejiang Normal University, Jinhua 321004 China (email: mingli@zjnu.edu.cn). Y. G. Wang is with Max Planck Institute for Mathematics in the Sciences, Leipzig, 04103 Germany, and also with the School of Mathematics and Statistics, The University of New South Wales, NSW, 2052 Australia (e-mail: yuguang.wang@unsw.edu.au).

X. Zheng and B. Zhou are the equal first contribution authors.

B. Zhou is the corresponding author.

Hadamard product of the projections.

Haar-based convolution alone, like other graph convolutions, cannot deal with graph-level classification when the input graph has different size and structure in the user-specified network architecture. To this end, we develop a Haar-based pooling operation to guarantee that the output of the network has a unified size. The Haar wavelet system for convolution is constructed from a coarse-grained tree of the input graph. Haar-based pooling provides a cascading computing strategy using this tree-structured system. It is thus a hierarchical design with multiple pooling layers. Each pooling layer compresses the node number by combining the feature values and graph topology of the current layer's input. Consequently, the implementation of pooling at the layer is simply a compressive Haar transform of the input feature.

In this paper, we propose a GNN using the above convolution and pooling; both defined in terms of the same graph Haar basis. As compared to existing GNNs, this strategy is distinguished in the following three aspects.

- **Efficient graph representation learning:** We generate coarse-grained tree structure for graphs to support fast computation on multiscale graph signal decomposition and cascading pooling workflow. The constructed orthogonal bases guarantee sufficient sparsity to capture mutual information between local and global embeddings with a low computational cost. Our method is not only capable of solving large-scale node-level learning problems, but also outstanding in handling graph-level problems.
- **Haar wavelet-based pooling strategy:** We develop a Haar wavelet method for the graph pooling computing. The fast transforms of Haar basis compress the node number, which can filter out the high-frequency information while preserving the major geometric and feature information of the input graph data. Due to the hierarchical construction of Haar wavelet system, our pooling scheme can naturally synthesize the spectral-based subgraph information and node feature.
- **End-to-end network architecture:** To the best of our knowledge, our method attempts for the first time to incorporate spectral-based convolutional and pooling layers in one GNN for graph classification and regression tasks. Haar basis can adequately represent both local and global information, and extract the topological and feature information of the graph data. Aside from theoretically appealing, empirical evidence supports the superiority of the proposed Haar-based GNN.

The rest of this paper is organised as follows. Section II reviews classic works of learning graph representation as well as recent developments. Section III introduces the fundamental ideas and notion that construct the spectral graph networks and Haar wavelet system. Section IV formulates the proposed Haar-based GNN method. In Section V, we test the proposed model on a variety of graph learning tasks, including both classification and regression tasks on benchmark and new data sets. Section VI summarises the paper together with a discussion on potential future work.

II. RELATED WORKS

Researchers have probed approaches for building the graph convolutional layers. Two representative types are spectral-based methods and spatial-based methods. The spectral graph convolution (SGC), introduced in [30], is based on convolution theorem and spectral graph theory [31]. SGC is realised based on the graph Fourier transforms (GFTs), which however suffers from the high computational complexity of the Laplacian eigendecomposition; and there is, in general, no fast implementation of GFTs due to the irregularity of the graph nodes.

On the other hand, filters in the Fourier domain cannot guarantee the localisation in the spatial (vertex) domain. ChebNet proposed in [32] uses Chebyshev polynomial approximation for graph convolution, which constructs a localised polynomial filter while circumventing the computation of the Laplacian eigendecomposition. GCN [33] simplifies ChebNet by using the first order Chebyshev polynomial of the graph Laplacian with renormalisation tricks in computation. Authors of [34], [35] develop wavelet-based GNNs by replacing GFTs with graph wavelet transforms (GWTs). Due to the high sparsity of wavelet basis matrix, GWTs are more computationally efficient than GFTs.

Compared with SGC, the spatial-based methods are closer to the conventional CNN convolution on image classification as the graph convolutions are computed based on a node's spatial relation and the learnable filters are defined in the vertex domain [36]–[40]. In particular, Gilmer et al. [26] provide the framework of message passing neural networks (MPNNs), encapsulating many existing GNNs in the viewpoint that information/message can be passed from one node to another along edges/paths directly.

While graph convolution layers aim at extracting high-level node representations, graph pooling layers are needed to obtain the graph-level representations, which are necessary for graph classification and regression problems as concerned in this work. The general process is to coarsen a graph into subgraphs, so that node representations on coarsened graphs represent higher graph-level representations, and then use a readout layer to collapse node representations of each graph into a unified graph representation. Authors of [26], [36], [41] extend the global sum/average pooling operations to graph models by simply summing or averaging all node features. Some advanced graph pooling methods, such as DiffPool [42], SortPool [43], TopKPool [44], [45], SAGPool [46], are proposed with special consideration on the hierarchical representations and the feature information. Apart from that, Noutahi *et al* [47] and Ma *et al* [48] take the graph Laplacian into account to combine the feature information and the structural information. Such spectral-based techniques drop the detailed information layer by layer to extract smoothing feature representations. Unfortunately, both methods have high computational cost mainly due to the Laplacian eigendecomposition.

III. TECHNICAL SUPPORTS

We define a set of input to be studied as $\Gamma = \{(\mathcal{G}_1, X_1), (\mathcal{G}_2, X_2), \dots, (\mathcal{G}_M, X_M)\}$ with graph \mathcal{G}_g and features X_g on it. A graph-level task aims at learning the hidden

representation for each graph (\mathcal{G}_g, X_g) to predict its label \mathcal{Y}_g in labels $\{\mathcal{Y}_1, \mathcal{Y}_2, \dots, \mathcal{Y}_M\}$. For an undirected and weighted graph instance $\mathcal{G}_g = (\mathcal{V}_g, \mathcal{E}_g, \mathcal{W}_g)$, the $\mathcal{V}_g = \{v_1, v_2, \dots, v_{N_g}\}$ is a non-empty finite set of $|\mathcal{V}_g| = N_g$ vertices, and $\mathcal{E}_g \subset \mathcal{V}_g \times \mathcal{V}_g$ is a set of edges that can be represented as a weighted adjacency matrix $\mathcal{W}_g \in \mathbb{R}^{N_g \times N_g}$.

A. Spectral Graph Convolution

The spectral method defines graph convolution by an orthogonal basis on the graph. For an arbitrary graph, a spectral convolution transforms the input signal X^{in} through the network trainable filter G

$$\begin{aligned} \tilde{X}^{\text{in}} &= X^{\text{in}}W; \\ X^{\text{out}} &= \sigma(\Phi G \Phi^{-1} \tilde{X}^{\text{in}}). \end{aligned} \quad (1)$$

where $\sigma(\cdot)$ is the non-linear activation function and Φ is the spectral basis matrix associated with the weighted adjacency matrix \mathcal{W} . The weight matrix $W \in \mathbb{R}^{d^{\text{in}} \times d^{\text{out}}}$ provides an affine transform of the input $X^{\text{in}} \in \mathbb{R}^{N \times d^{\text{in}}}$ to $\tilde{X}^{\text{in}} \in \mathbb{R}^{N \times d^{\text{out}}}$. A spectral convolution can be defined by (discrete) adjoint and forward spectral transforms: the adjoint spectral transform Φ^{-1} maps \tilde{X}^{in} from the vertex domain to the spectral domain; the filter G processes feature information by the Hadamard product with the transformed graph data; the forward spectral transform Φ transmits the information back to the vertex domain to accomplish the convolution. Here, we have used a weight detaching trick in Eq. (1), i.e., conducting feature transformation $X^{\text{in}}W$ before performing the graph convolution, to reduce the parameter complexity from $O(N \times d^{\text{in}} \times d^{\text{out}})$ to $O(N + d^{\text{in}} \times d^{\text{out}})$.

People have proposed many ways to generate spectral-based convolution. For example, graph Fourier transforms [49] define the transform matrix Φ by the graph Laplacian. Graph wavelet neural networks [34] use the graph wavelet transforms, which provides a sparse and localised convolution for GNN.

The network filter G plays a similar role as an image denoising task, where one uses low-pass filters to eliminate the noise in high frequencies. In GNNs, the network filter structure is data-driven and learned from the input graph data. The adaptivity to the data determines which part of the signals should be preserved, passed, or filtered out.

B. Coarse-grained Chain Encoder

Our graph convolution and graph pooling are based on a *coarse-grained chain* of the graph. We employ graph coarsening to construct the chain. The target of coarsening is to partition a graph \mathcal{G} into smaller meaningful clusters. By recursively downsampling vertices and creating new adjacent matrices, a hierarchical architecture is created to fold similar local features together. The clustering contributes to a chain of graphs. Each member at the layer coarser than the finest layer is a *coarse-grained graph* of its finer layer. The graph nodes from a coarser layer are called parents, and the nodes from a finer layer are called children.

To be precise, a coarse-grained chain is a sequence of graph

$$\mathcal{G}^{J \rightarrow J_0} := (\mathcal{G}^{(J)}, \mathcal{G}^{(J-1)}, \dots, \mathcal{G}^{(J_0)}),$$

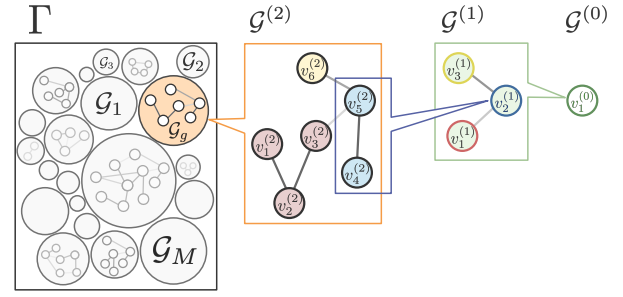


Fig. 2: The hierarchical relationship of graph data Γ , an individual graph \mathcal{G} and its coarse-grained graph $\mathcal{G}^{(j)}$ with $j = 0, 1, 2$ as a snapshot of coarse-grained chain. The level-wise Haar bases for every graph instance are generated from the constructed chain, and they are acting as the guidance of the corresponding graph convolution and graph pooling operations.

where $J > J_0$. In particular, we call $\mathcal{G}^{(J)}$ *the finest level* or *the bottom level* and it is inherited from the original graph. We recognise $\mathcal{G}^{(J_0)}$ as *the coarsest level* or *the top level*. The vertices at level j is denoted by

$$\mathcal{V}^{(j)} = \{v_1^{(j)}, \dots, v_{N^{(j)}}^{(j)}\},$$

where $N^{(j)} := |\mathcal{V}^{(j)}|$ indicates the number of vertices in graph $\mathcal{G}^{(j)}$. The complete chain structure can be constructed via either spectral or non-spectral clustering algorithms. Given the finest graph $\mathcal{G}^{(J)}$, we group $N^{(J)}$ vertices into $N^{(J-1)}$ clusters. Each cluster is a new vertex at the coarser level $\mathcal{G}^{(J-1)}$. The remaining coarser levels could be found accordingly until we reach the coarsest level $\mathcal{G}^{(J_0)}$. For any level j coarser than the finest, the k th vertex also represents the k th cluster of $\mathcal{G}^{(j+1)}$ and some cluster for any finer levels. Each $v_i^{(j+1)}$ at level $j+1$ from the k th cluster is called a *child* of the cluster, and $v_k^{(j)}$ at level j is the *parent* of all the elements in the same set.

There are many clustering methods, such as k -means [50], METIS [51] and spectral clustering [52]. By the time complexity, the METIS is faster than spectral clustering, which is faster than k -means. In terms of the clustering accuracy, spectral clustering and k -means are better than METIS. In practice, we will consider the trade-off between the computational cost and clustering precision.

C. Haar Orthonormal System and Local Filtration

Applying the conventional graph Fourier transform to GNNs is straight-forward and a conceptually important breakthrough. However, it comes with significant computational deficiency and lacks scalability. One way to overcome the computational intractability is to replace the Fourier basis by another orthonormal basis on the graph. The underlying orthonormal system should be feasible to compute while allowing efficient algorithms for spectral transforms. One such candidate is the Haar orthonormal basis introduced by [53]–[55].

Haar basis is a sparse orthogonal system that adapts to a coarse-grained chain of the underlying graph. To construct

the graph Haar basis, we form a hierarchical structure $\mathcal{G}^{J \rightarrow J_0}$ through progressively ‘folding’ the vertices of a graph. The local orthogonal system is then dilated along the chain until obtaining the global system at the bottom level, see Section IV for more details.

The Haar orthonormal system is completely constructive via a filtration (i.e. the chain). For the graph at each level of the coarse-grained chain, we establish an orthonormal basis. The basis at the finest layer becomes the global Haar basis of the underlying graph.

The Haar basis guarantees the orthogonality and locality of the system. The top-down procedure of basis generation creates a sparse yet non-redundant set of system, and the clustering of the chain connects the bases on two neighbouring layers of the chain. It with the locality sparsifies the Haar basis matrix and supports the feasibility of fast computation on scalable data. With such construction, the Haar system acquires the ability to handle graph input with changing size and structure. It naturally enables processing of different graphs with an embedded pooling operation, as we introduce below.

IV. THE PROPOSED HAARNET

We present our proposed model in this section. We focus on the model that works for graph classification and regression tasks. It includes three key operation blocks: orthogonal system construction, Haar graph convolution and hierarchical Haar graph pooling.

We first have a glance at the network architecture of our HaarNet model for graph classification and regression tasks, as illustrated in Fig. 4. As a typical GNN model, it contains Haar graph convolution, Haar graph pooling and fully connected layers in turn. Both the Haar graph convolution and pooling operations are defined by Haar Global Orthonormal Basis (HGOB) on an individual input graph \mathcal{G} . HGOB is fully constructive and based on a chain of the graph \mathcal{G} . The Haar graph convolution exploits the fast Haar transforms to extract the graph data in the Haar wavelet domain. The Haar graph pooling utilises the *compressive Haar transforms* filter out the high pass but keeps the low pass in the multi-resolution decomposition of the Haar wavelet system on the graph. In consequence of the tree structure of the Haar system, the graph size after the Haar pooling becomes identical, which enables the HaarNet to cope with graph samples with varying size and structure. We now introduce the computational principle for each unit of operation.

A. Global Orthonormal Basis

For the graph $\mathcal{G}^{(j)}$ of a chain at the j th layer, the constructed *Haar basis* is a set of $N^{(j)}$ vectors of length $N^{(j)}$. It forms a square matrix $\Phi^{(j)}$ of size $N^{(j)}$. By its nature, the Haar basis at each layer can be decomposed into ‘low-pass’ and ‘high-pass’:

$$\Phi^{(j)} = \begin{bmatrix} \Phi_{\text{low}}^{(j)} & \Phi_{\text{high}}^{(j)} \end{bmatrix}.$$

Here $\Phi_{\text{high}}^{(j)}$ can be generalised to multiple high passes. At the finest layer $\mathcal{G}^{(J)}$, we call $\Phi^{(J)}$ the *Haar global orthonormal*

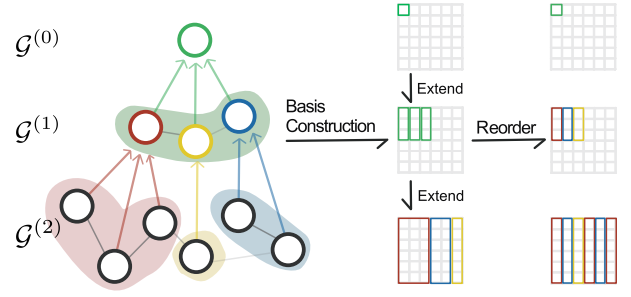


Fig. 3: A toy example of fast Haar basis construction. For a given graph \mathcal{G} , a bottom-up coarse-grained chain structure is first generated by clustering. The Haar global orthogonal basis is then constructed following a top-down fashion. Each parent basis at level j is dilated to level $j+1$. The number of dilated bases is determined by the number of its children at level $j+1$. The generated Haar basis is sparse and properly sorted. See Section IV-A for more details.

basis for the original graph \mathcal{G} , or simply *global Haar basis* for \mathcal{G} . The global Haar basis provides a multi-resolution decomposition and reconstruction, which is useful for sparsifying the pair-wise constant interaction in the input signal and reserving the mutual information between local and global embeddings [56].

The global Haar orthogonal basis has been studied extensively in [53]–[55], [57]. In particular, [54], [55], [57] show explicit construction and fast implementation for the Haar system. We aim at obtaining a sequence of the Haar orthogonal bases (matrices)

$$\{\Phi^{(J_0)}, \Phi^{(J_0+1)}, \dots, \Phi^{(J)}\},$$

where $\Phi^{(j)}$ is the basis matrix corresponding to the graph $\mathcal{G}^{(j)} = (\mathcal{V}^{(j)}, \mathcal{E}^{(j)}, \mathcal{W}^{(j)})$ at the j th level of the chain, which contains is composed of $N^{(j)}$ basis vectors

$$\Phi^{(j)} = (\phi_1^{(j)}, \phi_2^{(j)}, \dots, \phi_{N^{(j)}}^{(j)}).$$

The construction of the Haar system follows a top-down manner to recursively adopt the *characteristic function* and the *extension function* along the coarse-grained chain $\mathcal{G}^{J \rightarrow J_0} = (\mathcal{G}^{(J)}, \mathcal{G}^{(J-1)}, \dots, \mathcal{G}^{(J_0)})$. We start from preparing the node set $\mathcal{V}^{(j-1)} = \{v_1^{(j-1)}, \dots, v_{N^{(j)}}^{(j-1)}\}$ (which is ordered here for illustration simplicity) for the coarser level by sequencing the supernodes via their degrees or weights.

1) *Characteristic Function*: We define a characteristic function $\chi_k^{(j)}$ for the k th cluster in $\mathcal{V}^{(j)}$. It is also associated with the k th vertex $v_k^{(j-1)}$ in $\mathcal{V}^{(j-1)}$.

$$\chi_k^{(j)} := \begin{cases} 1, & v_i^{(c)} = v_k^{(j-1)}, \\ 0, & \text{otherwise.} \end{cases} \quad (2)$$

We use $\chi_k^{(j)} = 1$ to determine whether the vertex $v_i^{(j)}$ belongs to the k th cluster. The condition is equivalent to have a parent $v_k^{(j-1)}$ at the coarser $(j-1)$ th level.

2) *Extension Function*: The dimension of each Haar Basis is determined by the number of vertices at that level. Constructing $\Phi^{(j)}$ from $\Phi^{(j-1)}$ requires the size of the orthogonal system to be extended from $N^{(j-1)} \times N^{(j-1)}$ to $N^{(j)} \times N^{(j)}$. We achieve the target in the following two steps. We start from extending the column vectors $\{\phi_1^{(j-1)}, \dots, \phi_{N^{(j-1)}}^{(j-1)}\}$ vertically to obtain $N^{(j-1)}$ vectors of length $N^{(j)}$. The l th new basis, denoted by $\phi_l^{(j)*}$, is extended from

$$\phi_l^{(j)*} := \frac{\phi_l^{(j-1)}}{\sqrt{\xi_l^{(j)}}}, \quad (3)$$

where $\xi_l^{(j)}$ is the size of the l th cluster at level j . The vertices within the cluster share the same parent of $v_l^{(j-1)} \in \mathcal{V}^{(j-1)}$ at the coarser level $j-1$.

Next we apply the Gram-Schmidt process and extend the number of orthogonal basis to match the number of vertices at level j . Each $\phi_l^{(j)*}$ from Eq. (3) would be split into $\xi_l^{(j)}$ basis. For $k = 2, 3, \dots, \xi_l^{(j)}$, we define

$$\phi_{l,k}^{(j)} := \sqrt{\frac{\xi_l^{(j)} - k + 1}{\xi_l^{(j)} - k + 2}} \left(\chi_{k-1}^{(j)} - \frac{\sum_{i=k}^{\xi_l^{(j)}} \chi_{l,i}^{(j)}}{\xi_l^{(j)} - k + 1} \right). \quad (4)$$

Accumulating all $\phi_{l,k}^{(j)}$ together for all the l clusters, and we obtain an orthonormal basis for $\ell_2(\mathcal{G}^{(j)})$ at the j th layer from the $(j-1)$ th layer. The vectors of the basis gives the basis matrix $\Phi^{(j)} \in \mathbb{R}^{N^{(j)} \times N^{(j)}}$, which we call it a Haar transform on $\ell_2(\mathcal{G}^{(j)})$. For any chain structure $\mathcal{G}^{J \rightarrow J_0}$, we can always apply the ‘vertical extending - horizontal extending’ scheme and find the Haar orthogonal basis for the next finer level. When $j = J$, we reach the finest level and the corresponding $\Phi^{(J)}$ is called the *Haar Global Orthonormal Basis*, or HGOB, for the original graph \mathcal{G} .

One special case is the coarsest level J_0 , where each vertex belongs to an exclusive cluster, and there is no further coarser level ‘ J_{-1} ’. We modify Eq. (3) and Eq. (4) accordingly by defining $\phi_l^{(j-1)} = 1$ and $\xi_l^{(J_0)} = N^{(J_0)}$. For $l = 2, 3, \dots, N^{(J_0)}$, we have

$$\phi_1^{(J_0)} := \frac{1}{\sqrt{N^{(J_0)}}}$$

$$\phi_l^{(J_0)} := \sqrt{\frac{N^{(J_0)} - l + 1}{N^{(J_0)} - l + 2}} \left(\chi_{l-1}^{(J_0)} - \frac{\sum_{i=l}^{N^{(J_0)}} \chi_i^{(J_0)}}{N^{(J_0)} - l + 1} \right).$$

We now utilise the constructed bases $\{\phi_l^{(j)}\}_{l=1}^{N^{(j)}}$, $j = J_0, \dots, J$ on the chain to define a graph convolution and graph pooling, see Sections IV-B and IV-C.

B. Convolutional Layer

This section presents the motivation and details of the core operations in a Haar Convolutional Layer. We include the forward and adjoint Haar transforms for the Haar global orthonormal basis on the graph as constructed above, and their fast implementations as inspired by [35]. Also, we propose a padding strategy for training the global structure of filtration.

In this paper, instead of applying the Fourier basis, we use the Haar basis for the U in the graph convolution in Eq. (1). We rule out the Fourier basis of the graph Laplacian to avoid the fussy computation of a dense matrix. The computation cost of eigendecomposition and discrete Fourier transform increase dramatically with the graph size, which in no circumstance is desirable. In contrast, our Haar basis is constructed from the coarse-grained chain with clustering properties. The compressive workflow provides a sparsified operator Φ to support the fast computation of the adjoint and forward Haar transforms. We adopt the notation from the previous sections and detail the fast implementation below.

1) *Adjoint Haar Transform*: On level j of $\mathcal{G}_i^{(j)}$, the adjoint Haar transform formulates a set of *Haar coefficients* for X^{in}

$$(\Phi^{(j)})^T X^{\text{in}} = (c_1^{(j)}, \dots, c_{N^{(j)}}^{(j)}) \in \mathbb{R}^{N^{(j)} \times d}.$$

The l th coefficient with respect to $v_l^{(j)}$ is accumulated from its children vectors $v_{l'}^{(j)}$ at level $j+1$

$$c_l^{(j)} := \sum_{v_{l'}^{(j)} \in \mathcal{V}^{(j)}} \omega_l^{(j)} S_l^{(j)} \phi_{l'}^{(j)*} \quad (5)$$

$$\omega_l^{(j)} := \frac{1}{\sqrt{\xi_l^{(j)}}} \quad (6)$$

$$S_l^{(j)} := \sum_{v_{l'}^{(j+1)} \in v_l^{(j)}} \omega_{l'}^{(j+1)} S_{v_{l'}}^{(j+1)}. \quad (7)$$

In a nutshell, the coefficient $c_l^{(j)}$ for $v_l^{(j)}$ reflects the weighted sum of information from its children. The *weight factors* for each child is defined by Eq. (6), and the recursive summation follows Eq. (7).

2) *Forward Haar Transform*: The forward Haar transform sends the Haar coefficients back to the vertex domain. Given a set of coefficients $c = \{c_1, \dots, c_N\}$ at the finest level $\mathcal{G}^{(J)}$, the reconstruction is, for $l = 1, \dots, N$,

$$\Phi c_l := \sum_{j=J_0}^J W_l^{(j)} \left(\sum_{k=N^{(j-1)}+1}^{N^{(j)}} c_k \phi_{k_j}^{(j)*} \right) \quad (8)$$

$$W_l^{(j)} := \prod_{k=J_0}^j \frac{1}{\omega_k^{(j)}} \quad \text{for } j = J_0, \dots, J-1. \quad (9)$$

For a vertex $v_k^{(J)}$, we accumulate weighted information from its parents $v_{k_j}^{(j)}$ at each coarser level j for $j = J_0, \dots, J-1$. The weight factor $\omega_k^{(j)}$ follows the same format as in Eq. (6).

3) *Padding Strategy*: The trainable filter matrix G is learned in the wavelet domain and it is used to process the Haar coefficients. Conventionally, the matrix for an individual graph $\mathcal{G}^{(j)}$ is constructed as a diagonal matrix of size $N^{(j)}$. In graph-level tasks, different graphs share the same number of features, but contain varying number of nodes. To eliminate the inconsistency and apply an identical filtration rule along the full graph data set, we consider a padding strategy on Haar bases and extend all bases to a unified length. The modified basis matrix then has the form $\Phi^{(j)} \in \mathbb{R}^{N^{(j)} \times N_{\max}^{(j)}}$, $N_{\max}^{(j)} := \max\{N_1^{(j)}, \dots, N_M^{(j)}\}$, where we fill the extra columns by $\mathbf{0}$ vectors.

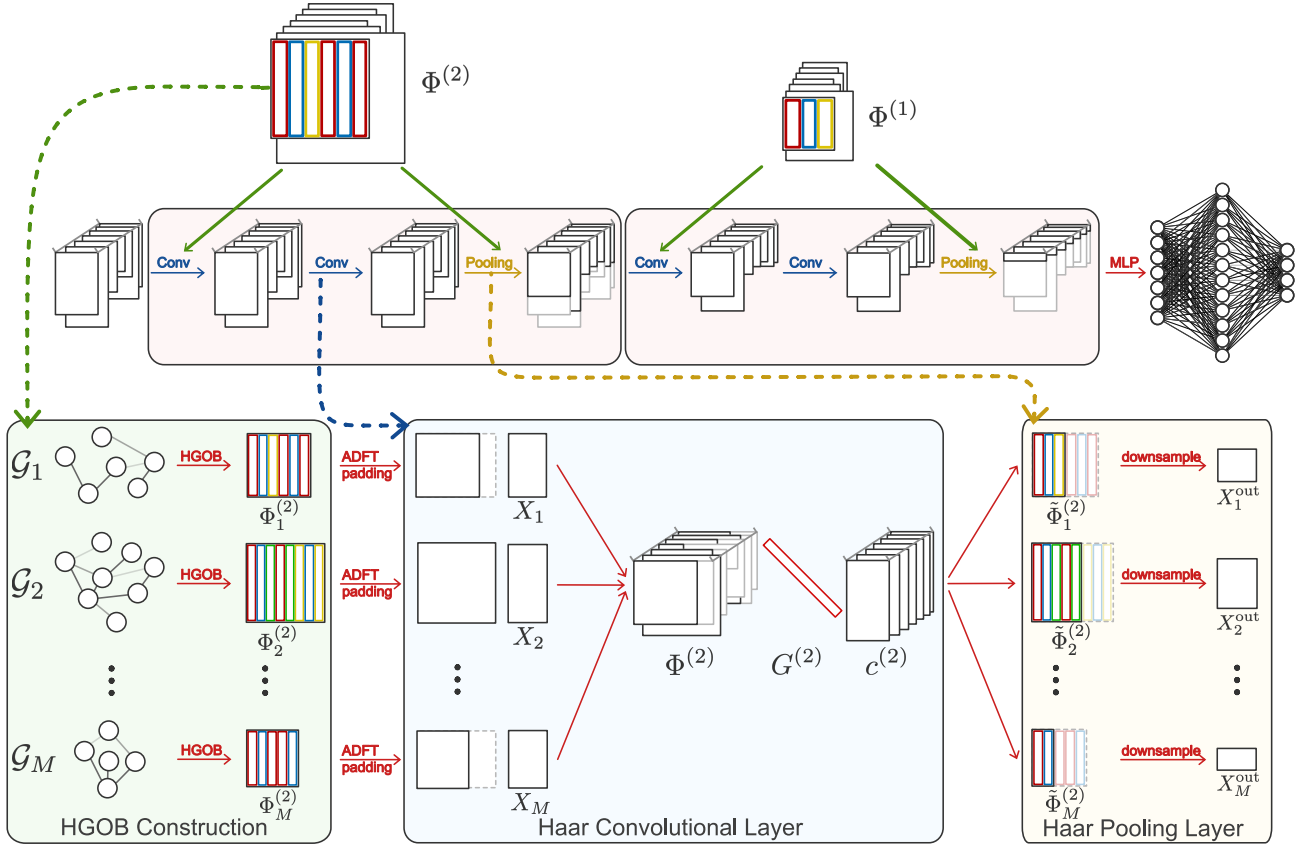


Fig. 4: An illustration of HAARNET structure with 2 Haar blocks and a fully connected layer. We unify a block of the HAARNET structure to cover Haar graph convolutional layer(s) following Haar graph pooling layer(s) (red rounded-rectangles). Given a set of graph Γ , we first construct the Haar basis sets $\Phi^{(2)}$ and $\Phi^{(1)}$ along the coarse-grained chain for each graph \mathcal{G}_i at level $j = 2$ and 1. The constructed orthonormal systems are applied to support convolutional and pooling operations. The formulations inside one Haar block only involves one basis set. For the first Haar block, we take the ordered HGObS $\Phi^{(2)} = \{\Phi_1^{(2)}, \Phi_2^{(2)}, \dots, \Phi_M^{(2)}\}$ to guide the adjoint and forward Haar transforms. The process, as detailed in the blue rounded-rectangle, constitutes one Haar graph convolutional layer. The filter matrix G is shared among graphs at the same level, and it is universally applicable on different graphs after the padding strategy on the Haar basis of Φ . For the sake of conciseness, we only demonstrate one convolutional layer. However, in practice, it could be repeated multiple times. We send the final output of the convolutional layer (after activation) to the pooling layer, where we utilise the compressive Haar transforms to filter out the high-pass signals and reserve low-pass signals. The coarsening process is implemented by the transform of $\Phi^{(2)}$; the $\Phi^{(1)}$ (yellow rounded-rectangles) gives the size of the output of the downsampling procedure. Note that the network component is not constrained to the illustration, and a specific application should determine the employed structure. For clarity, we also exclude some common technical details like activation and weight detaching in this visualization.

C. Pooling Layer

The well-constructed Haar Orthogonal System is applied to perform the pooling operation along the prepared coarse-grained chain. We summarize the motivation and key calculations. For more details we refer the readers to the technical analysis and proofs in [57]. For an input graph \mathcal{G} and its chain $\mathcal{G}^{J \rightarrow J_0}$, the *Haar pooling* consists of $J - J_0$ Haar pooling layers in the GNN. The Haar pooling of the j th layer is given by

$$\hat{X}^{(j)} = (\tilde{\Phi}^{(j)})^T X^{(j)} \quad (10)$$

for $j = J - 1, J - 2, \dots, J_0$, where $X^{(j)} \in \mathbb{R}^{N_{\max}^{(j)} \times d}$ is constituted from the output of the last convolutional layer. The

pooling operator $\tilde{\Phi}^{(j)}$ takes the first $N^{(j-1)}$ columns from the associated Haar Basis $\Phi^{(j)}$ at the level j of the chain. As a result, the output of this Haar Pooling layer downsamples the matrix size to $\mathbb{R}^{N^{(j-1)} \times d}$ for each graph. At the last Haar pooling layer, the output has a standard size $\mathbb{R}^{1 \times d'}$ for each graph. The output feature dimension d' is determined by the external weights of graph convolutional layers.

The compressive Haar transform follows a similar fast computational strategy as the adjoint transform in the convolutional layer. To minimise the number of summation and products operations, we modify the weighted sum of signal information in Eq. (7) by pre-gathering the feature vectors from child nodes to the coarsest possible level. Formally, for the input feature

$X^{(j)} \in \mathbb{R}^{N_{\max}^{(j)} \times d}$ at the j th layer, we prepare the weighted sum by

$$S^{(j)} := X^{(j)} \quad (11)$$

$$S_l^{(i)} := \sum_{v_{l'}^{(i+1)} \in v_l^{(i)}} \omega_{l'}^{(i+1)} S_{v_{l'}}^{(i+1)}. \quad (12)$$

We define $i \leq j$ to represent the coarsest possible layer where the corresponding $\phi_\ell^{(i)}$ is the ℓ th member of the orthonormal basis $\{\phi_\ell^{(i)}\}_{\ell=1}^{N^{(i)}}$. At each level j , the compressive Haar transform inherits full information from the first $N^{(j-1)}$ feature vectors which are elected as parent nodes at level $j-1$. The rest $N^{(j)} - N^{(j-1)}$ child nodes contribute their feature information to the coarsest possible layer. The information from parents and children are gathered via Eq. (11) and Eq. (12), respectively. The calculation of weights $\omega_{l'}^{(i+1)}$ follows Eq. (6), and the final result of the compressive Haar transform is then given by Eq. (5).

The pooling operation is essential to our graph regression and classification tasks. It unifies graph embedding for a given set of graphs with different structure and sizes. Such unanimity allows our model to handle graph data without further pre-processing. Besides, adopting Haar Pooling layers benefits our GNN from three particular perspectives. First, it takes only the low-frequency coefficients to approximate the original data. The noise in high-frequency coefficients are stripped out, and the remaining information is adequately purified. As a result of performing local graph Fourier transformation, the subgraph structure and the node features are utilised for generating the supernode representations. As pointed out by [43], [58], the compound information maximises the model performance. Also, [56], [57] have shown that the Haar basis is closely related to the average pooling operation, which incorporates the spatial behaviour of the graph signal. Such pooling strategy has attested its power in many practical applications of CNN and GNN.

V. EXPERIMENTAL STUDY

In this section, we evaluate our proposed framework HAARNET on several graph classification and regression tasks. In Part V-B, we select four popular graph classification data sets and compare the performance of our HAARNET with some representative methods in the literature. Also, we demonstrate the capability of learning on a large-scale data set for our proposed method with a multi-class classification task in Part V-C. Finally, we present one regression task in Part V-D. We present the partial descriptive statistics of all the data sets used in this paper in TABLE I, and provide detailed descriptions in the corresponding subsections.

All the programs in this work were written in PyTorch [59] and the library PyTorch Geometric [60], and all the experiments run on NVIDIA® Tesla V100 GPU with 5,120 CUDA cores and 16GB HBM2 mounted on a high performance computing cluster.

A. Experimental Setup

For each data set, we tune the model architecture of our proposed HAARNET to produce the best performance. The

architecture search is conducted based on the number of pooling operations and the number of convolutional layers before each pooling operation. A two- or three-layer multilayer perceptron (MLP) is used as the classifier after the sequence of convolutional and pooling layers across all the experiments. The best architecture of HAARNET for each data set is reported in the corresponding subsections. We employ spectral clustering [61], [62] to generate the coarse-grained chain with a given number of tree layers. Spectral clustering has a provable capability of clustering various data patterns and can also handle the graph with isolated nodes.

We split the data set in each experiment into training, validation and test sets by 80%, 10% and 10% respectively. As noticed in [63], different data splits will affect the performance of a GNN model to a great extent. Thus, we repeat each experiment 10 times with random shuffling for the data set before splitting. Note that there is also randomness involved in the spectral clustering step, which leads to a slightly different coarse-grained chain generated for each graph. To rule out this unwanted randomness, we pre-process each data set and attach the generated coarse-grained chain with associated Haar bases. Therefore, the random shuffling will not affect the structures of the coarse-grained chains.

We report the mean accuracy (or loss in the regression task) and the standard deviation of our model in all experiments. For the baseline methods in Part V-B, unless otherwise specified, we only report the best-published results from their corresponding original papers for the available data sets. For Parts V-C and V-D, we will specify the sources where the results of the baseline methods are retrieved.

We use the Adam optimizer [64] with an early stopping criterion as suggested in [63]. Specifically, we set a maximum of 150 epochs and stop training if the validation loss does not improve for consecutive 25 epochs. For the tasks in Parts V-C and V-D, we turn off the early stopping, and the experiment runs for a 20 and 100 epochs respectively. We leverage Tune [65] and HyperOpt [66] to perform the parallel hyperparameter tuning. We document a list of the hyperparameters of the model in TABLE II along with their search spaces.

B. Graph Classification Benchmarks

In this part, we test the proposed HAARNET on four graph classification benchmarks, and compare its performance with traditional graph kernel methods and recent existing GNN models.

We give the selected benchmark data sets as follows. **D&D** [67], [68] is a protein graph data set consisting of a collection of protein structures. A graph represents each protein in the data set. The nodes are amino acids, and an edge connects two nodes if they are less than six angstroms apart. The node features of each graph are the binary encoding of some chemical properties. The task is to classify the protein structures into enzymes and non-enzymes; **PROTEINS** [67], [69] is also a protein structure data set which we consider as a simplified version of **D&D** with the same task. The protein structures documented in **PROTEINS** are much smaller than in **D&D** in terms of the node and edge numbers. **MUTAG**

TABLE I: Statistical information of the data sets used for graph classification and regression tasks.

Data sets	PROTEINS	ENZYMES	D&D	MUTAG	PointPattern(0.30)*	PointPattern(0.35)*	PointPattern(0.40)*	QM7**
Max. #Nodes	620	126	5,748	28	1,000	1,000	1,000	23
Min. #Nodes	4	2	30	10	100	100	100	4
Avg. #Nodes	39.06	32.63	284.32	17.93	478	474	475	15.44
Avg. #Edges	72.82	62.14	715.66	19.79	1632.50	1611.50	1610.00	122.83
#Graphs	1,113	600	1,178	188	15,000	15,000	15,000	7,165
#Classes	2	6	2	2	3	3	3	1

*The number included in the bracket indicates the type of the PointPattern data set, and the level of difficulty of the task. The meaning of this number will be explained in Part V-D.

**The data set is used for the regression task and the #Classes represents number of regression targets.

TABLE II: Grid search space for the hyperparameters used in all the experiments.

Hyperparameter	Choice
Learning rate	1e-2, 5e-3, 1e-3, 5e-4, 1e-4
Hidden size	16, 32, 64, 128
Weight decay (L2)	5e-3, 1e-3, 5e-4, 1e-4
Batch size	32, 64, 128, 256
#Poolings	1, 2, 3

[70], [71] is a mutagen data set comprising 188 compounds. Each compound is represented by a graph where atoms are nodes, and covalent bonds are edges. The task is to predict whether a compound in the data set is mutagenic based on its compound structure and chemical properties. **ENZYMES** [69], [72] is a graph data set consisting of 100 proteins. The proteins will be classified into six Enzymes Commission top-level enzyme classes (EC classes), such as oxidoreductases (EC1) and transferases (EC2). It is thus a multi-class graph classification task.

To demonstrate the performance of our proposed HAARNET on these four benchmark classification data sets, we consider the following state-of-the-art methods as the baselines:

- GIN [38] generalizes the Weisfeiler-Lehman graph isomorphism test and thus achieves maximum discriminative power among the class of GNNs.
- PATCHYSAN [73] uses a receptive field for the nodes and extracts locally connected regions from graphs.
- DGCNN [43] proposes the so-called SortPooling layer and applies convolution on the sorted graph nodes.
- DIFFPOOL [42] learns a soft assignment matrix by a separate pooling GNN module. The learned assignment matrix is then used to transform the node embeddings and the graph structure.
- SAGPOOL [46] develops a pooling layer based on self-attention mechanism using graph convolution. SAGPOOL takes into account both node features and graph structure.
- EIGENPOOL [48] is a spectral pooling method which

relies on graph Fourier transform. They employ the traditional GCN [33] for graph convolution and form a complete framework for graph representation learning.

- G-U-NETS [44] is an encoder-decoder architecture which involves the proposed graph pooling (gPool) and unpooling (gUnpool) procedures.
- We also compare with several graph kernel methods, including Shortest-Path kernel (SP) [74], GRAPHLET count kernel [75], random walk kernel (RW) [76] and Weisfeiler-Lehman subtree kernel (WL) [68].

The model architectures of our HAARNET used in **PROTEINS** and **MUTAG** are two Haar convolutional (HaarConv) layers followed by one Haar pooling (HaarPool) layer and a three-layer MLP. The architecture used in **D&D** and **ENZYMES** are two HaarConv layers followed by one HaarPool layer and a two-layer MLP as the classifier. For each of these tasks, we apply batch normalization [77] for all layers of MLP, except for the output layer.

We summarize the results in TABLE III. Overall, our proposed HAARNET obtains a superior performance against the baselines on all the data sets. For **PROTEINS** and **D&D**, HAARNET achieves the top test accuracy. For **ENZYMES** and **MUTAG**, the performance of our HAARNET is ranked top-three among all the baselines. It demonstrates that our proposed model can effectively extract global topological information of input graph via a hierarchical learning process, and can adequately capture latent node clustering information by the chain-based sparse Haar representation.

Moreover, we exploit the t-distributed Stochastic Neighbor Embedding (t-SNE) to visualize the test classification results of the pre-trained classifier on **PROTEINS** and **D&D**. (We exclude **ENZYMES** and **MUTAG** due to the limited number of test samples in these two data sets.) We use a two-dimensional embedding space for visualization, and the point in the embedding space corresponds to a graph of the test set. Fig. 5 suggests that there is a visible clustering pattern of the graphs processed by the sequence of HaarConv and HaarPool layers in our model.

C. Large Data Set for Point Distribution Recognition

There are many benchmark graph data sets used in the related literature for graph classification tasks, see [78], [79] for examples. However, many data sets still suffer from a lack

TABLE III: Mean test accuracy (in percentage) and standard deviation of HAARNET as compared with existing models on benchmark graph classification data sets, over 10 repetitions.

Methods	PROTEINS	ENZYMES	D&D	MUTAG
SP	75.07*	42.32 ^a	—	85.79*
GRAPHLET	71.67*	41.03 ^a	78.45*	81.58*
RW	74.22*	—	—	83.68*
WL	72.92*	53.43 ^a	77.95*	80.72*
GIN	76.2	—	—	89.4
PATCHYSAN	75.00	—	76.27	91.58
DGCNN	75.54	57.12 ^a	79.37	85.83
DIFFPOOL	76.25	62.53^a	80.64	—
SAGPOOL	72.17	—	77.07	—
EIGENPOOL	76.6	65.0	78.6	—
G-U-NETS	77.68	—	82.43	—
HAARNET	78.3±1.60	62.5±3.85	82.5±3.59	89.6±2.49

*' denotes the record retrieved from PATCHYSAN [73].

'a' denotes the record retrieved from DIFFPOOL [42].

'—' means that the record is not available in the corresponding papers.

! The decimal place is not modified when transferring the results.

! The **best** result is in **bold**, and the **second** and **third** positions are marked in **red** and **blue**, respectively.

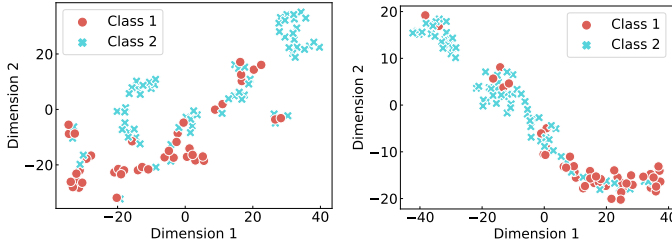


Fig. 5: t-SNE visualizations on test set. The points denote the graphs, and the different colors represent the true class labels. Left: **PROTEINS**. Right: **D&D**.

of understanding of the underlying mechanism, which may lead to an unexplainable graph representation generated from a graph learning method.

We introduce a novel large-scale graph classification data set composed of simple point patterns from the statistical mechanics. We simulate three types of point patterns in two-dimensional space: hard disks in equilibrium (HD), Poisson point process (PPP) and random sequential adsorption (RSA) of disks. The PPP and HD are the models that are typically used to describe the micro-structures of gases and liquids [80]. The RSA is a non-equilibrium stochastic process which simulates the particles one by one with some satisfied non-overlapping conditions. The point patterns simulated by these three mechanics are structurally different; thus, a collection of these point patterns forms a graph classification task with the three simulation models being the class labels. Each point pattern is represented as a graph, where the particles are reviewed as nodes, and there is an edge connecting two nodes if the two particles are within a threshold distance. The node degree is used as the feature for each node of all the graphs. We name the resulting data set as **PointPattern**. Compared to the data sets used in Part V-B, **PointPattern** is large-scale in terms of sample size, graph size, and the number of connections within each graph.

The volume fraction covered by particles ϕ_{HD} of HD is fixed at 0.5, and this factor for the point pattern simulated from PPP is $\phi_{PPP} = 0$. Moreover, we can tune the corresponding factor ϕ_{RSA} of the RSA model to control the similarity between RSA and the other two simulation models. If ϕ_{RSA} becomes closer to 0.5, it is harder to distinguish the point patterns RSA from HD. Hence, the factor ϕ_{RSA} can be used to adjust the level of difficulty of the task. In this experiment, we consider three data sets with varying levels of difficulty $\phi_{RSA} = \{0.30, 0.35, 0.40\}$.

We compare our proposed HAARNET with the following two GNN baselines: GCNCONV+TOPKPOOL uses GCN [33] convolutional layer with TopK [44], [45] pooling layer; GINCONV+TOPKPOOL employs GIN [38] convolutional layer with TopK [44], [45] pooling layer. All the models, including our HAARNET share the same neural architecture: three units of alternating convolutional layer and pooling layer followed by a three-layer MLP. We apply the dropout [81] only for the first layer of MLP in each model to prevent from over-fitting. In GCNCONV+TOPKPOOL and GINCONV+TOPKPOOL, we use global max pooling to unify the graph representations before feeding to the MLP classifier. In this experiment, we fix the number of hidden neurons to 64, learning rate to 0.001 and weight decay to 0.0005 for all the models. Each **PointPattern** data set is a 3-classification task on 15,000 graphs (5,000 for each class) with graph node size varying between 100 and 1,000. We refer the reader to TABLE I for more statistics of the data sets. The data split and other experimental settings are the same as the procedures described in Part V-A. The experiment results are reported in TABLE IV and Fig. 6.

From the results in TABLE IV, we can see that our HAARNET outperforms the baselines GCNCONV+TOPKPOOL and GINCONV+TOPKPOOL on each of three data sets by a large margin with 5 to 7 percentage points higher mean test accuracy. Moreover, HAARNET also achieves much smaller standard deviations than the baseline methods across all the data sets. We further compare the trends of validation loss and accuracy against epoch of the proposed HAARNET to those of the baselines in Fig. 6. Although HAARNET has a higher validation loss during the first 2 epochs than the baseline methods, it converges rapidly and reaches the stationary point within 7 epochs in training each data set. Fig. 6 also shows that HAARNET obtains much smaller variations in term of validation loss and validation accuracy. The lower validation loss, higher validation accuracy and higher test accuracy of our HAARNET on all the data sets indicate the superior learning and generalization abilities. Based on these observations, we can conclude that the proposed HAARNET is a highly effective and robust model for large-scale graph classification tasks.

D. Graph Regression

In this part, we evaluate the performance of the HAARNET on a graph regression task with **QM7** data set [82], [83] from the field of quantum chemistry. The data set consists of 7,165 molecules, each of which contains up to 23 atoms. We represent each molecule by a graph with the atoms as nodes and bonds as edges. Then, the Coulomb energy matrix

TABLE IV: Mean test accuracy (in percentage) and standard deviation of HAARNET and the other two baseline models on **PointPattern** with three different levels of difficulty ϕ_{RSA} . The test accuracy is averaged over 10 repetitions each with 20 epochs and different random seeds.

PointPattern	GINCONV + SAGPOOL	GCNCONV + TOPKPOOL	HAARNET
$\phi_{\text{RSA}} = 0.30$	90.9 \pm 2.95	92.9 \pm 3.21	97.4\pm0.34
$\phi_{\text{RSA}} = 0.35$	86.7 \pm 3.30	89.3 \pm 3.31	96.0\pm0.59
$\phi_{\text{RSA}} = 0.40$	80.2 \pm 3.80	85.1 \pm 4.06	92.7\pm0.72

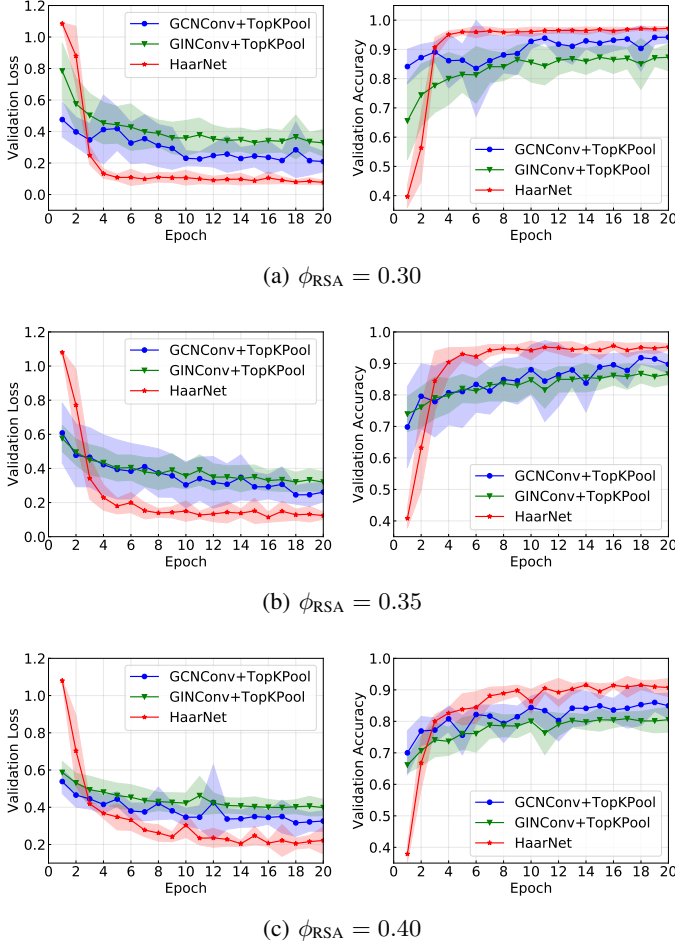


Fig. 6: The plots of validation loss against epoch and validation accuracy against epoch for **PointPattern** with three different levels of difficulty $\phi_{\text{RSA}} = \{0.30, 0.35, 0.40\}$.

of each molecule becomes the adjacency matrix which depicts the topological structure of the corresponding graph. The atomization energy value of the molecule is the regression label. Since the atom itself is featureless, we create an uninformative feature (i.e., constant scalar 1) for each node of all the graphs. Under this construction, the regressor model will only leverage the structure of the graphs.

In the experiment, we standardize the target values for the training procedure and then convert the predicted value back to the original domain for evaluating the model on the validation and test sets. As suggested in [26], we use mean squared error (MSE) as the metric for the training and mean absolute error

(MAE) for the evaluations. To validate the capability of our model, we borrow the following baselines along with their records directly from [29] for comparison: Random Forest (RF) [84], Multitask Networks (MULTITASK) [85], Kernel Ridge Regression (KRR) [86], and Graph Convolutional models (GC) [87]. To make more comparison, we test on the model with convolution plus pooling unit GCNCONV+SAGPOOL. We employ one GCN [33] convolutional layer followed by one widely used graph pooling layer SAGPOOL [46] and a three-layer multilayer perceptron (MLP) as the classifier. The neural architecture of our HAARNET is identical to the baseline GCNCONV+SAGPOOL.

TABLE V: Average of test mean absolute error (MAE) and standard deviation over 10 repetitions on **QM7** for the graph regression task.

Methods	Test MAE
RF	122.7 \pm 4.2*
MULTITASK	123.7 \pm 15.6*
KRR	110.3 \pm 4.7*
GC	77.9 \pm 2.1*
GCNCONV+SAGPOOL	43.6 \pm 0.98
HAARNET (Ours)	42.7\pm0.92

*' indicates the records retrieved from [29].

TABLE V shows the results of the experiment. The HAARNET achieves the lowest mean test MAE among all the baselines, which demonstrate the superior performance of our proposed method on this regression task. Compared to the baseline GCNCONV+SAGPOOL model, HAARNET not only obtains an even lower mean test MAE but also has a slightly smaller standard deviation (calculated in the same number of repetitions and epochs). These observations confirm that our proposed HAARNET is an effective and robust model for graph regression task.

VI. CONCLUSION

We proposed HAARNET for graph classification and regression tasks. It is an end-to-end graph neural network with interrelated graph convolutional and graph pooling layers. The HaarNet model learns efficient graph representation in the convolution and unified topological information in the pooling. In comparison to existing approaches, our method manages to preserve both local and global information while making maximal use of extracted mutual information. Our spectral-based method is supported by robust novel theories and also

achieves superior prediction accuracy and stable performance in extensive experiments. Evidence proves that our method outperforms its competitors, especially on large-scale data sets.

We left some potentials for future study. First, the expressivity power of the model is worth exploring. While empirical results have shown its capability, a rigorous theoretical analysis on the expressivity of HAARNET could help to solidify the usefulness not only for our framework but also potentially for general spectral-based methods. Also, although we test our model mostly on the well-explored benchmark data sets, it could as well be useful for real-world applications, such as building knowledge graphs for drug repositioning for COVID-19. Besides, the design of graph clustering needs to investigate further. It is not yet clear to what extent the clustering methods would have an impact on the performance of our proposed HAARNET, and what is the guideline of choosing the clustering methods that could better capture graph topological information. Since the coarse-grained chain is built upon the clustering results, methods that encode specific edge-connection patterns could be an extra benefit to our model.

REFERENCES

- [1] M. M. Bronstein, J. Bruna, Y. LeCun, A. Szlam, and P. Vandergheynst, "Geometric deep learning: Going beyond Euclidean data," *IEEE Signal Processing Magazine*, vol. 34, no. 4, pp. 18–42, July 2017.
- [2] W. L. Hamilton, R. Ying, and J. Leskovec, "Representation learning on graphs: Methods and applications," *IEEE Data Engineering Bulletin*, 2017.
- [3] P. W. Battaglia, J. B. Hamrick, V. Bapst, A. Sanchez-Gonzalez, V. Zambaldi, M. Malinowski, A. Tacchetti, D. Raposo, A. Santoro, R. Faulkner et al., "Relational inductive biases, deep learning, and graph networks," *arXiv:1806.01261*, 2018.
- [4] S. Casas, C. Gulino, R. Liao, and R. Urtasun, "Spatially-aware graph neural networks for relational behavior forecasting from sensor data," in *ICRA*, 2020.
- [5] B. Perozzi, R. Al-Rfou, and S. Skiena, "Deepwalk: Online learning of social representations," in *KDD*, 2014, pp. 701–710.
- [6] D. Teney, L. Liu, and A. van Den Hengel, "Graph-structured representations for visual question answering," in *CVPR*, 2017, pp. 1–9.
- [7] Y. Wang, Y. Sun, Z. Liu, S. E. Sarma, M. M. Bronstein, and J. M. Solomon, "Dynamic graph CNN for learning on point clouds," *ACM Transactions On Graphics (TOG)*, vol. 38, no. 5, pp. 1–12, 2019.
- [8] D. M. Bear, C. Fan, D. Mrowca, Y. Li, S. Alter, A. Nayebi, J. Schwartz, L. Fei-Fei, J. Wu, J. B. Tenenbaum et al., "Learning physical graph representations from visual scenes," *arXiv:2006.12373*, 2020.
- [9] R. Ying, R. He, K. Chen, P. Eksombatchai, W. L. Hamilton, and J. Leskovec, "Graph convolutional neural networks for web-scale recommender systems," in *KDD*, 2018, pp. 974–983.
- [10] J. Ji, R. Krishna, L. Fei-Fei, and J. C. Niebles, "Action genome: Actions as compositions of spatio-temporal scene graphs," in *CVPR*, 2020, pp. 10 236–10 247.
- [11] M. Gori, G. Monfardini, and F. Scarselli, "A new model for learning in graph domains," in *IJCNN*, vol. 2. IEEE, 2005, pp. 729–734.
- [12] A. Micheli, "Neural network for graphs: A contextual constructive approach," *IEEE Transactions on Neural Networks*, vol. 20, no. 3, pp. 498–511, 2009.
- [13] F. Scarselli, M. Gori, A. C. Tsoi, M. Hagenbuchner, and G. Monfardini, "The graph neural network model," *IEEE Transactions on Neural Networks*, vol. 20, no. 1, pp. 61–80, 2008.
- [14] —, "Computational capabilities of graph neural networks," *IEEE Transactions on Neural Networks*, vol. 20, no. 1, pp. 81–102, 2008.
- [15] J. Zhou, G. Cui, Z. Zhang, C. Yang, Z. Liu, L. Wang, C. Li, and M. Sun, "Graph neural networks: A review of methods and applications," *arXiv:1812.08434*, 2018.
- [16] Z. Zhang, P. Cui, and W. Zhu, "Deep learning on graphs: A survey," *IEEE Transactions on Knowledge and Data Engineering*, 2020, DOI: 10.1109/TKDE.2020.2981333.
- [17] Z. Wu, S. Pan, F. Chen, G. Long, C. Zhang, and S. Y. Philip, "A comprehensive survey on graph neural networks," *IEEE Transactions on Neural Networks and Learning Systems*, 2020, DOI: 10.1109/TNNLS.2020.2978386.
- [18] H. M. Berman, J. Westbrook, Z. Feng, G. Gilliland, T. N. Bhat, H. Weissig, I. N. Shindyalov, and P. E. Bourne, "The Protein Data Bank," *Nucleic Acids Research*, vol. 28, no. 1, pp. 235–242, 01 2000. [Online]. Available: <https://doi.org/10.1093/nar/28.1.235>
- [19] X. Shen, Q. Dai, S. Mao, F.-I. Chung, and K.-S. Choi, "Network together: Node classification via cross-network deep network embedding," *IEEE Transactions on Neural Networks and Learning Systems*, 2020.
- [20] D. Domingo-Fernández, S. Baksi, B. Schultz, Y. Gadiya, R. Karki, T. Raschka, C. Ebeling, M. Hofmann-Apitius, and A. T. Kodumullil, "COVID-19 knowledge graph: a computable, multi-modal, cause-and-effect knowledge model of COVID-19 pathophysiology," *bioRxiv*, 2020. [Online]. Available: <https://www.biorxiv.org/content/early/2020/04/15/2020.04.14.040667>
- [21] T. Kipf, E. Fetaya, K.-C. Wang, M. Welling, and R. Zemel, "Neural relational inference for interacting systems," in *ICML*, 2018.
- [22] V. N. Ioannidis, X. Song, S. Manchanda, M. Li, X. Pan, D. Zheng, X. Ning, X. Zeng, and G. Karypis, "DRKG – Drug repurposing knowledge graph for Covid-19," <https://github.com/gnn4dr/DRKG/>, 2020.
- [23] M. Zhang and Y. Chen, "Link prediction based on graph neural networks," in *NeurIPS*, 2018, pp. 5165–5175.
- [24] J. Jiang, C. Xu, Z. Cui, T. Zhang, W. Zheng, and J. Yang, "Walk-steered convolution for graph classification," *IEEE Transactions on Neural Networks and Learning Systems*, 2019.
- [25] X. Zhang, C. Xu, X. Tian, and D. Tao, "Graph edge convolutional neural networks for skeleton-based action recognition," *IEEE Transactions on Neural Networks and Learning Systems*, 2019.
- [26] J. Gilmer, S. S. Schoenholz, P. F. Riley, O. Vinyals, and G. E. Dahl, "Neural message passing for quantum chemistry," in *NeurIPS*, vol. 70, 2017, pp. 1263–1272.
- [27] Z. Ma, M. Li, and Y. G. Wang, "PAN: Path integral based convolution for deep graph neural networks," *ICML Workshop on Learning and Reasoning with Graph-Structured Representations*, 2019.
- [28] Z. Ma, J. Xuan, Y. G. Wang, M. Li, and P. Lio, "Path integral based convolution and pooling for graph neural networks," *arXiv:2006.16811*, 2020.
- [29] Z. Wu, B. Ramsundar, E. N. Feinberg, J. Gomes, C. Geniesse, A. S. Pappu, K. Leswing, and V. Pande, "MoleculeNet: A benchmark for molecular machine learning," *Chemical Science*, vol. 9, no. 2, pp. 513–530, 2018.
- [30] J. Bruna, W. Zaremba, A. Szlam, and Y. LeCun, "Spectral networks and locally connected networks on graphs," *arXiv:1312.6203*, 2013.
- [31] F. R. Chung and F. C. Graham, *Spectral Graph Theory*. American Mathematical Society, 1997, no. 92.
- [32] M. Defferrard, X. Bresson, and P. Vandergheynst, "Convolutional neural networks on graphs with fast localized spectral filtering," in *NeurIPS*, 2016, pp. 3844–3852.
- [33] T. N. Kipf and M. Welling, "Semi-supervised classification with graph convolutional networks," in *ICLR*, 2017.
- [34] B. Xu, H. Shen, Q. Cao, Y. Qiu, and X. Cheng, "Graph wavelet neural network," in *ICLR*, 2019. [Online]. Available: <https://openreview.net/forum?id=H1ewdiR5tQ>
- [35] M. Li, Z. Ma, Y. G. Wang, and X. Zhuang, "Fast Haar transforms for graph neural networks," *Neural Networks*, 2020, DOI: <https://doi.org/10.1016/j.neunet.2020.04.028>
- [36] J. Atwood and D. Towsley, "Diffusion-convolutional neural networks," in *NeurIPS*, 2016, pp. 1993–2001.
- [37] P. Velickovi, G. Cucurull, A. Casanova, A. Romero, P. Li, and Y. Bengio, "Graph attention networks," in *ICLR*, 2018. [Online]. Available: <https://openreview.net/forum?id=rJXmpikCZ>
- [38] K. Xu, W. Hu, J. Leskovec, and S. Jegelka, "How powerful are graph neural networks?" in *ICLR*, 2019. [Online]. Available: <https://openreview.net/forum?id=ryGs6iA5Km>
- [39] W. Hamilton, Z. Ying, and J. Leskovec, "Inductive representation learning on large graphs," in *NeurIPS*, 2017, pp. 1024–1034.
- [40] F. Monti, D. Boscaini, J. Masci, E. Rodola, J. Svoboda, and M. M. Bronstein, "Geometric deep learning on graphs and manifolds using mixture model cnns," in *CVPR*, 2017, pp. 5115–5124.
- [41] D. K. Duvenaud, D. Maclaurin, J. Iparraguirre, R. Bombarell, T. Hirzel, A. Aspuru-Guzik, and R. P. Adams, "Convolutional networks on graphs for learning molecular fingerprints," in *NeurIPS*, 2015, pp. 2224–2232.
- [42] Z. Ying, J. You, C. Morris, X. Ren, W. Hamilton, and J. Leskovec, "Hierarchical graph representation learning with differentiable pooling," in *NeurIPS*, 2018, pp. 4800–4810.

- [43] M. Zhang, Z. Cui, M. Neumann, and Y. Chen, "An end-to-end deep learning architecture for graph classification," in *AAAI*, 2018.
- [44] H. Gao and S. Ji, "Graph u-nets," in *ICML*, 2019.
- [45] C. Cangea, P. Veličković, N. Jovanović, T. Kipf, and P. Liò, "Towards sparse hierarchical graph classifiers," *NeurIPS Workshop on Relational Representation Learning*, 2018.
- [46] J. Lee, I. Lee, and J. Kang, "Self-attention graph pooling," in *ICML*, 2019.
- [47] E. Noutahi, D. Beani, J. Horwood, and P. Tossou, "Towards interpretable sparse graph representation learning with laplacian pooling," *arXiv:1905.11577*, 2019.
- [48] Y. Ma, S. Wang, C. C. Aggarwal, and J. Tang, "Graph convolutional networks with eigenpooling," in *KDD*, 2019, pp. 723–731.
- [49] D. I. Shuman, S. K. Narang, P. Frossard, A. Ortega, and P. Vandergheynst, "The emerging field of signal processing on graphs: Extending high-dimensional data analysis to networks and other irregular domains," *IEEE Signal Processing Magazine*, vol. 30, no. 3, pp. 83–98, 2013.
- [50] S. Lloyd, "Least squares quantization in PCM," *IEEE Transactions on Information Theory*, vol. 28, no. 2, pp. 129–137, 1982.
- [51] G. Karypis and V. Kumar, "A fast and high quality multilevel scheme for partitioning irregular graphs," *SIAM Journal on Scientific Computing*, vol. 20, no. 1, pp. 359–392, 1998.
- [52] U. Von Luxburg, "A tutorial on spectral clustering," *Statistics and Computing*, vol. 17, no. 4, pp. 395–416, 2007.
- [53] M. Gavish and R. R. Coifman, "Sampling, denoising and compression of matrices by coherent matrix organization," *Applied and Computational Harmonic Analysis*, vol. 33, no. 3, pp. 354–369, 2012.
- [54] C. Chui, F. Filbir, and H. Mhaskar, "Representation of functions on big data: graphs and trees," *Applied and Computational Harmonic Analysis*, vol. 38, no. 3, pp. 489–509, 2015.
- [55] Y. G. Wang and X. Zhuang, "Tight framelets on graphs for multiscale data analysis," in *Wavelets and Sparsity XVIII*, vol. 11138. International Society for Optics and Photonics, 2019, p. 111380B.
- [56] J. C. Ye, Y. Han, and E. Cha, "Deep convolutional framelets: A general deep learning framework for inverse problems," *SIAM Journal on Imaging Sciences*, vol. 11, no. 2, pp. 991–1048, 2018.
- [57] Y. G. Wang, M. Li, Z. Ma, G. Montufar, X. Zhuang, and Y. Fan, "Haar graph pooling," in *ICML*, 2020.
- [58] C. Morris, K. Kersting, and P. Mutzel, "Glocalized Weisfeiler-Lehman graph kernels: Global-local feature maps of graphs," in *ICDM*, 2017, pp. 327–336.
- [59] A. Paszke, S. Gross, F. Massa, A. Lerer, J. Bradbury, G. Chanan, T. Killeen, Z. Lin, N. Gimelshein, L. Antiga, A. Desmaison, A. Kopf, E. Yang, Z. DeVito, M. Raison, A. Tejani, S. Chilamkurthy, B. Steiner, L. Fang, J. Bai, and S. Chintala, "Pytorch: An imperative style, high-performance deep learning library," in *NeurIPS*, 2019, pp. 8024–8035.
- [60] M. Fey and J. E. Lenssen, "Fast graph representation learning with PyTorch Geometric," *ICLR Workshop on Representation Learning on Graphs and Manifolds*, 2019.
- [61] J. Shi and J. Malik, "Normalized cuts and image segmentation," *IEEE Transactions on Pattern Analysis and Machine Intelligence*, vol. 22, no. 8, pp. 888–905, 2000.
- [62] X. Y. Stella and J. Shi, "Multiclass spectral clustering," in *ICCV*, 2003, pp. 313–319 vol.1.
- [63] O. Shchur, M. Mumme, A. Bojchevski, and S. Günnemann, "Pitfalls of graph neural network evaluation," *NeurIPS Workshop on Relational Representation Learning*, 2018.
- [64] D. P. Kingma and J. Ba, "Adam: A method for stochastic optimization," in *ICLR*, Y. Bengio and Y. LeCun, Eds., 2015.
- [65] R. Liaw, E. Liang, R. Nishihara, P. Moritz, J. E. Gonzalez, and I. Stoica, "Tune: A research platform for distributed model selection and training," *ICML Workshop on Automated Machine Learning*, 2018.
- [66] J. Bergstra, D. Yamins, and D. D. Cox, "Making a science of model search: Hyperparameter optimization in hundreds of dimensions for vision architectures," in *ICML*, 2013, pp. 115–123.
- [67] P. D. Dobson and A. J. Doig, "Distinguishing enzyme structures from non-enzymes without alignments," *Journal of Molecular Biology*, vol. 330, no. 4, pp. 771–783, 2003.
- [68] N. Shervashidze, P. Schweitzer, E. J. Van Leeuwen, K. Mehlhorn, and K. M. Borgwardt, "Weisfeiler-Lehman graph kernels," *Journal of Machine Learning Research*, vol. 12, no. 77, pp. 2539–2561, 2011.
- [69] K. M. Borgwardt, C. S. Ong, S. Schönauer, S. Vishwanathan, A. J. Smola, and H.-P. Kriegel, "Protein function prediction via graph kernels," *Bioinformatics*, vol. 21, no. suppl_1, pp. i47–i56, 2005.
- [70] A. K. Debnath, R. L. Lopez de Compadre, G. Debnath, A. J. Shusterman, and C. Hansch, "Structure-activity relationship of mutagenic aromatic and heteroaromatic nitro compounds. correlation with molecular orbital energies and hydrophobicity," *Journal of Medicinal Chemistry*, vol. 34, no. 2, pp. 786–797, 1991.
- [71] N. Kriege and P. Mutzel, "Subgraph matching kernels for attributed graphs," in *ICML*, 2012.
- [72] I. Schomburg, A. Chang, C. Ebeling, M. Gremse, C. Heldt, G. Huhn, and D. Schomburg, "Brenda, the enzyme database: updates and major new developments," *Nucleic Acids Research*, vol. 32, no. suppl_1, pp. D431–D433, 2004.
- [73] M. Niepert, M. Ahmed, and K. Kutzkov, "Learning convolutional neural networks for graphs," in *ICML*, 2016, pp. 2014–2023.
- [74] K. M. Borgwardt and H.-P. Kriegel, "Shortest-path kernels on graphs," in *ICDM*. IEEE, 2005, pp. 74–81.
- [75] N. Shervashidze, S. Vishwanathan, T. Petri, K. Mehlhorn, and K. Borgwardt, "Efficient graphlet kernels for large graph comparison," in *AIS-TATS*, 2009, pp. 488–495.
- [76] T. Gärtner, P. Flach, and S. Wrobel, "On graph kernels: Hardness results and efficient alternatives," in *Learning Theory and Kernel Machines*. Springer, 2003, pp. 129–143.
- [77] S. Ioffe and C. Szegedy, "Batch normalization: Accelerating deep network training by reducing internal covariate shift," in *ICML*, 2015.
- [78] V. P. Dwivedi, C. K. Joshi, T. Laurent, Y. Bengio, and X. Bresson, "Benchmarking graph neural networks," *arXiv:2003.00982*, 2020.
- [79] W. Hu, M. Fey, M. Zitnik, Y. Dong, H. Ren, B. Liu, M. Catasta, and J. Leskovec, "Open Graph Benchmark: Datasets for machine learning on graphs," *arXiv:2005.00687*, 2020.
- [80] J.-P. Hansen and I. R. McDonald, *Theory of Simple Liquids*. Elsevier, 1990.
- [81] G. E. Hinton, N. Srivastava, A. Krizhevsky, I. Sutskever, and R. R. Salakhutdinov, "Improving neural networks by preventing co-adaptation of feature detectors," *arXiv:1207.0580*, 2012.
- [82] L. C. Blum and J.-L. Reymond, "970 million druglike small molecules for virtual screening in the chemical universe database GDB-13," *Journal of the American Chemical Society*, vol. 131, p. 8732, 2009.
- [83] M. Rupp, A. Tkatchenko, K.-R. Müller, and O. A. von Lilienfeld, "Fast and accurate modeling of molecular atomization energies with machine learning," *Physical Review Letters*, vol. 108, p. 058301, 2012.
- [84] L. Breiman, "Random forests," *Machine Learning*, vol. 45, no. 1, pp. 5–32, 2001.
- [85] B. Ramsundar, S. Kearnes, P. Riley, D. Webster, D. Konerding, and V. Pande, "Massively multitask networks for drug discovery," *arXiv:1502.02072*, 2015.
- [86] C. Cortes and V. Vapnik, "Support-vector networks," *Machine Learning*, vol. 20, no. 3, pp. 273–297, 1995.
- [87] H. Altae-Tran, B. Ramsundar, A. S. Pappu, and V. Pande, "Low data drug discovery with one-shot learning," *ACS Central Science*, vol. 3, no. 4, pp. 283–293, 2017.